Tellus (2000), 52A, 129–139
Printed in UK. All rights reserved

TELLUS
ISSN 0280–6495

A proposed adiabatic formulation of 3-dimensional global atmospheric models based on potential vorticity

By YONG LI[1]*, J. RUGE[2], J. R. BATES[3] and A. BRANDT[4], [1]*Data Assimilation Office and Joint Center for Earth System Technology, NASA/Goddard Space Flight Center, Greenbelt, Maryland 20771, USA;* [2]*Front Range Scientific Computation, and University of Colorado, USA;* [3]*University of Copenhagen, Copenhagen, Denmark;* [4]*Weizmann Institute of Science, Israel*

(Manuscript received 22 December 1998; in final form 5 October 1999)

ABSTRACT

A 2-time-level finite difference atmospheric general circulation model based on the semi-Lagrangian advection of pseudo potential vorticity (which becomes potential vorticity in that part of the domain where the hybrid vertical coordinate becomes isentropic) has been formulated. At low levels, the hybrid vertical coordinate is terrain following. The problem of isentropic potential vorticity possibly becoming ill-defined in the regions of planetary boundary layer is thus circumvented. The divergence equation is a companion to the (pseudo) potential vorticity equation and the model is thus called a PV-D model. Many features of a previously developed shallow water PV-D model are carried over: a modification of the PV equation needed to give computational stability of long Rossby waves; a semi-Lagrangian semi-implicit treatment of both the linear and the nonlinear terms; the use of an unstaggered grid in the horizontal; the use of a nonlinear multigrid technique to solve the nonlinear implicit equations. A linear numerical stability analysis of the model's gravity–inertia waves indicates that the potential temperature needs to be separated into horizontal mean and perturbation parts. This allows an implicit treatment of the vertical advection associated with the mean in the thermodynamic equation. Numerical experiments with developing baroclinic waves have been carried out and give realistic results.

1. Introduction

Potential vorticity (PV), being conserved following a particle in frictionless adiabatic flow, is a basic quantity in atmospheric dynamics. Since its discovery by Rossby (1936) in the shallow water context and by Ertel (1942) for general flows, it has frequently been used as an analytical and diagnostic tool. In recent years, following the landmark paper of Hoskins et al. (1985), PV has received increased attention and its use in diagnostic studies has been leading to many new insights into atmospheric behaviour.

In view of the central importance of PV as a dynamical quantity, it would appear worthwhile to attempt to formulate an atmospheric model in which PV appears explicitly as a prognostic variable. It is reasonable to assume that such a model will give a more faithful simulation of PV evolution than one using the velocity components or vorticity and divergence as the primary prognostic variables. A step towards the development of such a model was taken by Charney (1962) for the shallow water case. Charney used the PV equation in conjunction with a balanced form of the divergence equation and showed that successful integrations could be carried out. Temperton and

* Corresponding author address: Data Assimilation Office, NASA/Goddard Space Flight Center, Code 910.3, Greenbelt, MD 20771, USA.
e-mail: lyong@dao.gsfc.nasa.gov

Staniforth (1987) took this approach a step further by formulating a limited-area PV-based model using the form of the shallow water equations.

We have been engaged in a project aimed at developing a global PV-based model using the primitive equations. Work on the shallow water version, has already been completed (Bates et al., 1995; Li and Bates, 1996). Our approach is to use the PV equation in conjunction with the primitive divergence equation, and our model is thus termed a PV-D model. A number of factors have made it opportune to embark on the development of such a model. The semi-Lagrangian method of integration, which has been gaining increasing implementations since it was first used in primitive equation models in the early 1980s (Robert, 1981, 1982; Bates and McDonald, 1982; for a review see Staniforth and Côté, 1991), offers high accuracy of integration and is ideally suited to the numerical treatment of quantities that follow a conservation law along a particle trajectory. Multigrid methods, which provide an efficient means of solving the nonlinear implicit equations that arise in a PV-D model, are reaching a high state of development (Brandt, 1977, 1988; McCormick, 1992). The potential of isentropic coordinates, which are apposite for a PV-D model in 3-dimensions, has been demonstrated for the primitive equations (Hsu and Arakawa, 1990; Zhu et al., 1992; Johnson et al., 1993; Bleck and Benjamin, 1993). A recent formulation of a generalized vertical coordinate by Konor and Arakawa (1997) allows the use of a terrain following coordinate such as the commonly used σ-coordinate at the lower levels and smoothly changes to isentropic above. This suits our PV-D model development well, as will be seen later in this paper. An important factor motivating the continued development of our PV-D model is the demonstration that a PV-D model can be used conveniently as a tool for assimilating data on PV proxies, such as long-lived chemical tracers in the stratosphere (Li et al., 1998).

Other work on developing global PV-based models has also been carried out recently. Tolstykh (1996) has developed a semi-Lagrangian shallow water model using 4th order finite differencing, and Thuburn (1997) has developed an Eulerian shallow water model using a hexagonal–icosahedral grid.

In the present paper, we describe an adiabatic formulation of a 3-dimensional PV-D model. In considering an extension of our shallow water PV-D model to the 3D case, the approach that first suggested itself was to use the advection of Ertel PV (Ertel, 1942). This, however, is not a viable approach as the Ertel PV can become singular in regions of neutral vertical stratification that often occurs in the planetary boundary layer. To overcome this problem, we use a hybrid vertical coordinate (terrain following near the ground and smoothly changing to isentropic at higher levels) and derive a pseudo potential vorticity (PPV) equation, which reduces to the PV equation in regions where the vertical coordinate becomes isentropic. The divergence equation is derived, as in the shallow water case, by first discretizing the momentum equation in vector form and then taking the divergence. This gives an equation which is linear in the implicit variables. The thermodynamic equation is expressed in the form of conservation of potential temperature. A modification to the basic advection scheme needed to keep the gravity–inertia waves stable is introduced. The remaining equations are the hydrostatic equation and the continuity equation.

Many features of our shallow water PV-D model are carried over to the present case. The modification to the PV equation needed to keep the long Rossby waves stable is used, as is the 2-time-level semi-Lagrangian semi-implicit (SLSI) treatment of both the linear and the nonlinear terms. The price of the SLSI treatment of the nonlinear terms is the necessity of solving a nonlinear set of implicit equations. This is done, as in the shallow water case, by using a nonlinear multigrid solver. Our model uses a regular latitude–longitude grid, with no staggering of the variables. In the vertical, we use a type of staggered grid which seems best adapted to the present model. It follows Charney and Phillips (1953) more closely than Lorenz (1960).

2. Model formulation

2.1. *The continuous equations*

We use a generalized vertical coordinate ξ which is assumed to increase monotonically with height (Kasahara, 1974). The primitive equations for a dry atmosphere, i.e., the horizontal momentum equation, the hydrostatic equation, the continuity equation and the thermodynamic equation, can

be written as:

$$\frac{\mathrm{d}\boldsymbol{V}}{\mathrm{d}t} + f\boldsymbol{k} \times \boldsymbol{V} = \boldsymbol{P}, \tag{1}$$

$$\frac{\partial M}{\partial \xi} - c_{\mathrm{p}}\Pi \frac{\partial \theta}{\partial \xi} = 0, \tag{2}$$

$$\frac{\mathrm{d}}{\mathrm{d}t}\left(\frac{\partial p}{\partial \xi}\right) + \left(\frac{\partial p}{\partial \xi}\right)\left(\nabla \cdot \boldsymbol{V} + \frac{\partial \dot{\xi}}{\partial \xi}\right) = 0, \tag{3}$$

$$\frac{\mathrm{d}\theta}{\mathrm{d}t} = 0 \tag{4}$$

where

$\boldsymbol{V}$ = horizontal velocity vector ($= u\boldsymbol{i} + v\boldsymbol{j}$),
θ = potential temperature,
p = pressure,
ξ = vertical coordinate,
$\dot{\xi}$ = vertical velocity ($\mathrm{d}\xi/\mathrm{d}t$),
M = Montgomery streamfunction ($c_{\mathrm{p}}T + \Phi$),
Φ = geopotential,
f = Coriolis parameter,
c_{p} = specific heat of dry air at constant pressure,
p_{00} = reference pressure,
R_{d} = gas constant for dry air,
$\kappa = R_{\mathrm{d}}/c_{\mathrm{p}}$,
$\boldsymbol{P}$ = pressure gradient force
$(= -\nabla_{\xi} M + c_{\mathrm{p}}\Pi\nabla_{\xi}\theta)$,
$\Pi = (p/p_{00})^{\kappa}$.

From the horizontal momentum eq. (1) we derive the vorticity equation

$$\frac{\mathrm{d}}{\mathrm{d}t}(\zeta + f) + (\zeta + f)\nabla \cdot \boldsymbol{V} + \boldsymbol{k} \cdot \left(\nabla\dot{\xi} \times \frac{\partial \boldsymbol{V}}{\partial \xi}\right) = \boldsymbol{k} \cdot \nabla \times \boldsymbol{P}. \tag{5}$$

Using (3) to eliminate $\nabla \cdot \boldsymbol{V}$ from (5), we have

$$\frac{\mathrm{d}}{\mathrm{d}t}\left[-\frac{\zeta + f}{\partial p/\partial \xi}\right] = g_1, \tag{6}$$

where

$$g_1 = -\frac{1}{\partial p/\partial \xi}\left[(\zeta + f)\frac{\partial \dot{\xi}}{\partial \xi} + \boldsymbol{k} \cdot \left(\nabla \times \boldsymbol{P} + \frac{\partial \boldsymbol{V}}{\partial \xi} \times \nabla\dot{\xi}\right)\right]. \tag{7}$$

We call the quantity $[-(\zeta + f)/\partial p/\partial \xi]$ pseudo potential vorticity (PPV)* and eq. (6) the PPV equation. When the vertical coordinate becomes isentropic (i.e., $\xi = \theta$), as is intended except near the lower boundary, the pseudo potential vorticity becomes Ertel potential vorticity. Clearly, all the terms on the right-hand side of eq. (6) vanish in this case (assuming frictionless adiabatic flow). In the lower layers where the vertical coordinate is chosen to be σ, PPV is still well-defined. Therefore, by using (6), the difficulty of the PV being ill-defined is avoided, and the original intent of using the conservation relation for PV as a model equation is retained for most of the model domain. The form of ξ will follow Konor and Arakawa (1997) closely.

As in Bates *et al.* (1995), the divergence equation is obtained by discretizing the momentum equation in vector form and then taking the divergence. The last equation needed to close the system is derived from the definition of the vertical coordinate:

$$\xi(p, p_{\mathrm{s}}, \theta) = \xi. \tag{8}$$

2.2. *Semi-Lagrangian semi-implicit discretization*

The model equations are discretized in a 2-time-level semi-Lagrangian semi-implicit (SLSI) manner with 1st-order uncentering (Rivest et al., 1994), which can be extended to 2nd order with very little effort.

The discretization of the PPV eq. (6) starts from

$$\frac{1}{\Delta t}\left[\left(\frac{\zeta + f}{\partial p/\partial \xi}\right)^{n+1} - \left(\frac{\zeta + f}{\partial p/\partial \xi}\right)_{*}^{n}\right] = -\frac{1}{2}\left[(1 + \varepsilon)(g_1)^{n+1} + (1 - \varepsilon)(g_1)_{*}^{n}\right], \tag{9}$$

where ε is the uncentering parameter and Δt the timestep. The superscripts denote the timelevel, and the subscript $(\,)_*$ denotes quantities valued at the departure points. (Note that uncentering occurs only when ξ is not isentropic; when $\xi = \theta$, the r.h.s. in (9) vanishes.) In order to stabilize the Rossby waves, the modification to the Coriolis term as described in Bates et al. (1995) and the uncentering method of Li and Bates (1996) that

* It is not to be confused with quasi-geostrophic potential vorticity, which is also sometimes called pseudo potential vorticity.

suppresses the orographic resonance while imposing no damping effects on Rossby waves are adopted; this gives

$$f_* = f\left(1 - \frac{1}{2}\left[\frac{v_*^n \Delta t}{a}\right]^2\right) - \beta\left(\frac{v^{n+1} + v_*^n}{2}\right)\Delta t, \tag{10}$$

where a is the radius of the earth and $\beta = (1/a)\,\partial f/\partial\phi$. Hence, defining $\tau_1 = \frac{1}{2}\Delta t(1+\varepsilon)$ and $\tau_2 = \frac{1}{2}\Delta t(1-\varepsilon)$, eq. (9) becomes:

$$\begin{aligned}\left[1 - \tau_1\left(\frac{\partial\dot{\xi}}{\partial\xi}\right)^{n+1}\right](\zeta + f)^{n+1} &= \tau_1 \boldsymbol{k}\cdot\left[\nabla\times\boldsymbol{P} + \frac{\partial \boldsymbol{V}}{\partial\xi}\times\nabla\dot{\xi}\right]^{n+1} + \left(\frac{\partial p}{\partial\xi}\right)^{n+1} \\ &\times\left\{\frac{1}{(\partial p/\partial\xi)_*^n}\left[\zeta_*^n + f\left(1 - \frac{1}{2}\left[\frac{v_*^n\Delta t}{a}\right]^2\right)\right.\right. \\ &\left.\left. - \beta\left(\frac{v^{n+1} + v_*^n}{2}\right)\Delta t\right] - \tau_2(g_1)_*^n\right\}. \end{aligned} \tag{11}$$

The derivation of the divergence equation follows that of the shallow water PV-D model of Bates et al. (1995). We first discretize the momentum eq. (1) in vector form, giving

$$\left(\frac{\boldsymbol{V}^{n+1} - \boldsymbol{V}^n}{\Delta t}\right)_{\mathrm{H}} = \frac{1}{2}\left[(1+\varepsilon)(\boldsymbol{P} - f\boldsymbol{k}\times\boldsymbol{V})^{n+1} + (1-\varepsilon)(\boldsymbol{P} - f\boldsymbol{k}\times\boldsymbol{V})_*^n\right]_{\mathrm{H}}, \tag{12}$$

i.e.,

$$[\boldsymbol{V} - \tau_1(\boldsymbol{P} - f\boldsymbol{k}\times\boldsymbol{V})]_{\mathrm{H}}^{n+1} = [(\boldsymbol{V} + \tau_2(\boldsymbol{P} - f\boldsymbol{k}\times\boldsymbol{V}))_*^n]_{\mathrm{H}}, \tag{13}$$

where the subscript H denotes a horizontal projection as at the trajectory midpoint. Following Bates et al. (1990), (13) gives

$$[\boldsymbol{V} - \tau_1(\boldsymbol{P} - f\boldsymbol{k}\times\boldsymbol{V})]^{n+1} = \boldsymbol{A} \tag{14}$$

where

$$\boldsymbol{A} = A_\lambda \boldsymbol{i} + A_\phi \boldsymbol{j},$$

$$A_\lambda = \alpha_1(Y_\lambda)_*^n + \alpha_2(Y_\phi)_*^n,$$

$$A_\phi = \alpha_3(Y_\lambda)_*^n + \alpha_4(Y_\phi)_*^n,$$

$$Y_\lambda = u + \tau_2(P_\lambda + fv),$$

$$Y_\phi = v + \tau_2(P_\phi - fu),$$

and $(\alpha_1, \alpha_2, \alpha_3, \alpha_4)$ are defined as in Bates et al. (1990). Taking the divergence of (14), we arrive at the divergence equation

$$[D - \tau_1(\nabla\cdot\boldsymbol{P} - \beta u + f\zeta)]^{n+1} = \nabla\cdot\boldsymbol{A}, \tag{15}$$

where $D = \nabla\cdot\boldsymbol{V}$ is the divergence.

Discretizing the hydrostatic eq. (2) gives

$$\left(\frac{\partial M}{\partial\xi}\right)^{n+1} - c_{\mathrm{p}}\left[\Pi\frac{\partial\theta}{\partial\xi}\right]^{n+1} = 0. \tag{16}$$

The continuity eq. (3) is discretized as:

$$\begin{aligned}\frac{1}{\Delta t}\left[\left(\frac{\partial p}{\partial\xi}\right)^{n+1} - \left(\frac{\partial p}{\partial\xi}\right)_*^n\right] &= -\frac{1}{2}\left\{(1+\varepsilon)\left[\frac{\partial p}{\partial\xi}\left(D + \frac{\partial\dot{\xi}}{\partial\xi}\right)\right]^{n+1}\right. \\ &\left. + (1-\varepsilon)\left[\frac{\partial p}{\partial\xi}\left(D + \frac{\partial\dot{\xi}}{\partial\xi}\right)\right]_*^n\right\}, \end{aligned} \tag{17}$$

which can be re-written as:

$$\left[1 + \tau_1\left(D + \frac{\partial\dot{\xi}}{\partial\xi}\right)^{n+1}\right]\left(\frac{\partial p}{\partial\xi}\right)^{n+1} = \left[1 - \tau_2\left(D + \frac{\partial\dot{\xi}}{\partial\xi}\right)_*^n\right]\left(\frac{\partial p}{\partial\xi}\right)_*^n. \tag{18}$$

In order to maintain the numerical stability of gravity–inertia waves, as we will see later, we decompose the potential temperature into 2 parts, i.e., $\theta = \bar{\theta}(\xi) + \theta'(\lambda, \phi, \xi, t)$. Thus, eq. (4) becomes

$$\frac{\mathrm{d}\theta'}{\mathrm{d}t} + \Gamma\dot{\xi} = 0, \tag{19}$$

where $\Gamma = \partial\bar{\theta}/\partial\xi$. The SLSI discretization of this gives

$$[\theta' + \tau_1\Gamma\dot{\xi}]^{n+1} = [\theta' - \tau_2\Gamma\dot{\xi}]_*^n. \tag{20}$$

The definition of the vertical coordinate is itself one of the governing equations:

$$\xi[p^{n+1}, p_{\mathrm{s}}^{n+1}, \bar{\theta}(\xi) + (\theta')^{n+1}] = \xi. \tag{21}$$

With eqs. (11), (15), (16), (18), (20) and (21), we now have a closed set of governing equations.

2.3. *Vertical discretization and boundary conditions*

The vertical distribution of the model variables is illustrated in Fig. 1. Eqs. (11), (15), (18) are centered at the dashed levels, (20) at the solid

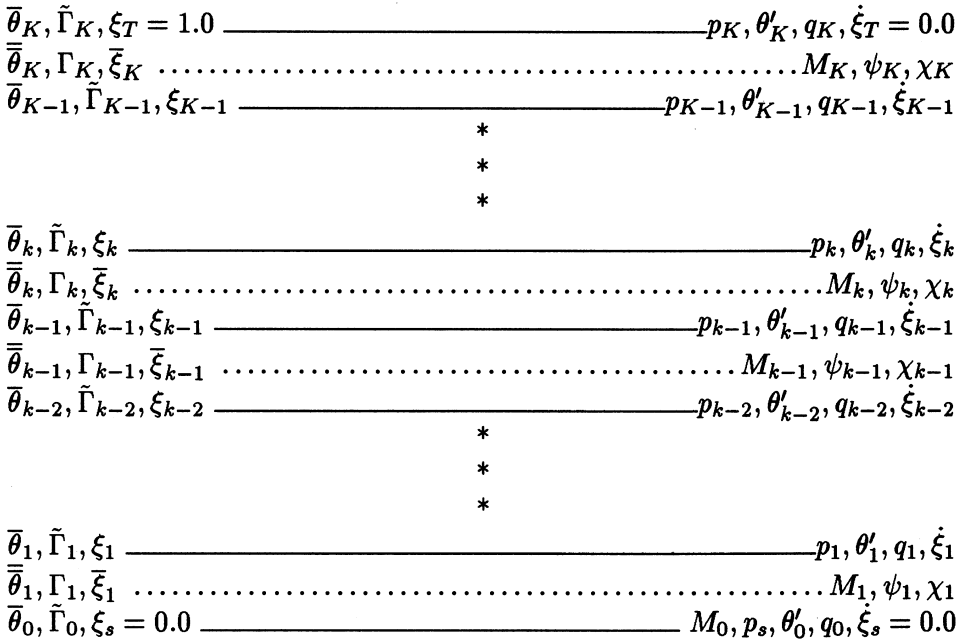

Fig. 1. The model's vertical grid. The meanings of the notations are as in the text.

levels, and (16) half way between the dashed levels (not the same as the solid levels when the grid is not uniform). This vertical grid follows Charney and Phillips (1953) more closely than Lorenz (1960). Therefore, the model is not subject to the computational noise usually associated with the Lorenz grid due to the extra degree of freedom in the vertical distribution of either the temperature (Arakawa and Konor, 1996) or the potential vorticity (Arakawa and Moorthi, 1988).

The boundary conditions at the bottom and the top of the model domain are as follows:

$$\dot{\xi}_0 = \dot{\xi}_K = 0, \tag{22}$$

$$M_0 = \Phi_s(\lambda, \phi) + c_p(\bar{\theta}_0 + \theta'_0)\left(\frac{p_s}{p_{00}}\right)^{\kappa}, \tag{23}$$

$$p_K = p_T(\lambda, \phi). \tag{24}$$

The pressure at the top has to be specified as a boundary condition, which in general is only approximate. But if the model has a few pressure levels at the top, which can be accommodated easily in this model, boundary condition (24) becomes exact.

3. Stability analysis

We carry out a stability analysis of the gravity–inertia waves with the linearized equations on the f-plane. For simplicity, we do it with the σ ($= 1 - p/p_s$) and the θ vertical coordinates, separately. We present here only the analysis with uniform grid. An extended analysis that allows a non-uniform grid has also been carried out; this does not alter the conclusions but is considerably more complicated. As for the numerical stability of Rossby waves, we use the method of treating the β-term implicitly as discussed in Bates et al. (1995). We present here the stability analysis in the σ-coordinate case in accord with the numerical results. A similar analysis in the θ-coordinate, confirming the numerical stability, will be presented in the future along with the correspondent numerical results.

In the case of the σ-coordinate, the model equations after being linearized about a state of rest are:

$$\left(\frac{\partial^2\psi'}{\partial x^2} - \frac{f_0}{\bar{p}_s}p'_s\right)^{n+1} - \left(\frac{\partial^2\psi'}{\partial x^2} - \frac{f_0}{\bar{p}_s}p'_s\right)^{n} = f_0\left[\tau_1\left(\frac{\partial\dot{\sigma}}{\partial\sigma}\right)^{n+1} + \tau_2\left(\frac{\partial\dot{\sigma}}{\partial\sigma}\right)^{n}\right], \tag{25}$$

$$\left(\frac{\partial^2\chi'}{\partial x^2}\right)^{n+1}-\left(\frac{\partial^2\chi'}{\partial x^2}\right)^{n}$$
$$=-\tau_1\left(\frac{\partial^2 M'}{\partial x^2}-c_{\mathrm{p}}\bar{\Pi}\frac{\partial^2\theta'}{\partial x^2}-f_0\frac{\partial^2\psi'}{\partial x^2}\right)^{n+1}$$
$$-\tau_2\left(\frac{\partial^2 M'}{\partial x^2}-c_{\mathrm{p}}\bar{\Pi}\frac{\partial^2\theta'}{\partial x^2}-f_0\frac{\partial^2\psi'}{\partial x^2}\right)^{n}, \qquad (26)$$

$$\left(\frac{\partial M'}{\partial\sigma}\right)^{n+1}=c_{\mathrm{p}}\bar{\Pi}\left(\frac{\partial\theta'}{\partial\sigma}\right)^{n+1}+\left(\frac{R_{\mathrm{d}}\bar{\Pi}\bar{\Pi}\Gamma}{\bar{p}}\right)(1-\sigma)(p_{\mathrm{s}}')^{n+1}, \qquad (27)$$

$$(p_{\mathrm{s}}')^{n+1}+\tau_1\bar{p}_{\mathrm{s}}\left(\frac{\partial^2\chi'}{\partial x^2}+\frac{\partial\dot{\sigma}'}{\partial\sigma}\right)^{n+1}=(p_{\mathrm{s}}')^{n}-\tau_2\bar{p}_{\mathrm{s}}\left(\frac{\partial^2\chi'}{\partial x^2}+\frac{\partial\dot{\sigma}'}{\partial\sigma}\right)^{n}, \qquad (28)$$

$$(\theta')^{n+1}-(\theta')^{n}+\Gamma[\tilde{\tau}_1(\dot{\sigma}')^{n+1}+\tilde{\tau}_2(\dot{\sigma}')^{n}+\tilde{\tau}_3(\dot{\sigma}')^{n+1}]=0, \qquad (29)$$

with ψ and χ meaning the streamfunction and velocity potential, and where $(\bar{\ })$ and $(\,)'$ denote the horizontal mean and the perturbation respectively. For eq. (29), $(\tilde{\tau}_1, \tilde{\tau}_2, \tilde{\tau}_3)$ are used in the place of (τ_1, τ_2) for the convenience of examining certain numerical stability properties, as will be seen later. It has been found (results not presented here) that using any monotonic function of σ as the vertical coordinate does not alter the conclusion of this stability analysis.

Assume that the solution takes the following form:

$$\begin{pmatrix}\psi'\\ \chi'\\ \theta'\\ M'\\ \dot{\sigma}'\\ p_{\mathrm{s}}'\end{pmatrix}^{n}=\begin{pmatrix}\hat{\psi}(\sigma)\\ \hat{\chi}(\sigma)\\ \hat{\theta}(\sigma)\\ \hat{M}(\sigma)\\ \hat{\sigma}(\sigma)\\ \hat{p}_{\mathrm{s}}\end{pmatrix}\Lambda^{n}\,\mathrm{e}^{imx}. \qquad (30)$$

Substituting (30) into eqs. (25)–(29) gives

$$-L\left[m^2\hat{\psi}(\sigma)+\frac{f_0}{\bar{p}_{\mathrm{s}}}\hat{p}_{\mathrm{s}}\right]=f_0\frac{\mathrm{d}\hat{\sigma}(\sigma)}{\mathrm{d}\sigma}, \qquad (31)$$

$$L\hat{\chi}(\sigma)=-\hat{M}(\sigma)+c_{\mathrm{p}}\bar{\Pi}\hat{\theta}(\sigma)+f_0\hat{\psi}(\sigma), \qquad (32)$$

$$\frac{\mathrm{d}\hat{M}(\sigma)}{\mathrm{d}\sigma}=c_{\mathrm{p}}\bar{\Pi}\frac{\mathrm{d}\hat{\theta}(\sigma)}{\mathrm{d}\sigma}+\left(\frac{R_{\mathrm{d}}\bar{\Pi}\Gamma}{\bar{p}}\right)(1-\sigma)\hat{p}_{\mathrm{s}}, \qquad (33)$$

$$L\hat{p}_{\mathrm{s}}=-\bar{p}_{\mathrm{s}}\left[-m^2\hat{\chi}(\sigma)+\frac{\mathrm{d}\hat{\sigma}(\sigma)}{\mathrm{d}\sigma}\right], \qquad (34)$$

$$L_1\hat{\theta}(\sigma)+\Gamma\hat{\sigma}(\sigma)=0, \qquad (35)$$

where

$$L=(\Lambda-1)/(\tau_1\Lambda+\tau_2)$$

and

$$L_1=(\Lambda-1)/(\tilde{\tau}_1\Lambda+\tilde{\tau}_2+\tilde{\tau}_3\Lambda^{-1}).$$

The above equations in vertically discretized form are (refer to Fig. 1 for the vertical positioning of the model variables):

$$-L\left[m^2\hat{\psi}_k+\frac{f_0}{\bar{p}_{\mathrm{s}}}\hat{p}_{\mathrm{s}}\right]=\left(\frac{f_0}{\Delta\sigma}\right)(\hat{\sigma}_k-\hat{\sigma}_{k-1}), \qquad (36)$$

$$L\hat{\chi}_k=-\hat{M}_k+\frac{1}{4}c_{\mathrm{p}}(\bar{\Pi}_k+\bar{\Pi}_{k-1})(\hat{\theta}_k+\hat{\theta}_{k-1})+f_0\hat{\psi}_k, \qquad (37)$$

$$\hat{M}_1=a_1(-5\hat{\theta}_0+6\hat{\theta}_1-\hat{\theta}_2)+b_1\hat{p}_{\mathrm{s}}+c_1\hat{\theta}_0$$
$$\hat{M}_k-\hat{M}_{k-1}=a_k(\hat{\theta}_k-\hat{\theta}_{k-2})+b_k\hat{p}_{\mathrm{s}},\qquad (k=2,3,4,\ldots,K), \qquad (38)$$

$$L\hat{p}_{\mathrm{s}}=-\bar{p}_{\mathrm{s}}\left[-m^2\hat{\chi}_k+\frac{1}{\Delta\sigma}(\hat{\sigma}_k-\hat{\sigma}_{k-1})\right], \qquad (39)$$

$$L_1\hat{\theta}_k+\tilde{\Gamma}_k\hat{\sigma}_k=0, \qquad (40)$$

where

$$c_1=-c_p\bar{\Pi}_0a_k+\begin{cases}c_p(3\bar{\Pi}_0+\bar{\Pi}_1)/32 & (k=1),\\ c_{\mathrm{p}}\bar{\Pi}_{k-1}/2 & (k=2,3,4,\ldots,K),\end{cases}$$

$$b_k=\begin{cases}[R_{\mathrm{d}}(3\bar{\Pi}_0+\bar{\Pi}_1)(\Gamma_1+\tilde{\Gamma}_0)(4-\Delta\sigma)\Delta\sigma]/[16(3\bar{p}_0+\bar{p}_1)]+R_{\mathrm{d}}\bar{\Pi}_0\bar{\theta}_0/\bar{p}_0, & (k=1),\\ [R_{\mathrm{d}}\bar{\Pi}_{k-1}\tilde{\Gamma}_{k-1}(1-\sigma_{k-1})\Delta\sigma]/[\bar{p}_{k-1}], & (k=2,3,4,\ldots,K),\end{cases}$$

$$c_1=-c_{\mathrm{p}}\bar{\Pi}_0.$$

Using (36), (39) and (40) to eliminate $\hat{\theta}$ and $\hat{\psi}$ from (37) gives:

$$(L+f_0^2L^{-1})\hat{\chi}_k = -\hat{M}_k - m^2L_1^{-1}[c_p(\bar{\Pi}_k+\bar{\Pi}_{k-1})\Delta\sigma/4] \times\left\{\tilde{\Gamma}_k\left[\sum_{k'=1}^{k}\hat{\chi}_{k'}-\frac{k}{K}\sum_{k'=1}^{K}\hat{\chi}_{k'}\right] +\tilde{\Gamma}_{k-1}\left[\sum_{k'=1}^{k-1}\hat{\chi}_{k'}-\frac{k-1}{K}\sum_{k'=1}^{K}\hat{\chi}_{k'}\right]\right\}. \quad (41)$$

This can be written in its matrix form as

$$(L+f_0^2L^{-1})\tilde{X} = -\tilde{M} - m^2L_1^{-1}C_\sigma\tilde{X}, \quad (42)$$

where C_σ is a matrix whose elements are determined by the vertical stratification of the basic state.

Using (39) and (40) to eliminate $\hat{p}_s$ and $\hat{\theta}$ from (38) gives:

$$\hat{M}_1 = m^2L_1^{-1}a_1\left[-6(\Delta\sigma)\tilde{\Gamma}_1\left(\hat{\chi}_1-\frac{1}{K}\sum_{k=1}^{K}\hat{\chi}_k\right) +(\Delta\sigma)\tilde{\Gamma}_2\left(\sum_{k'=1}^{2}\hat{\chi}_{k'}-\frac{2}{K}\sum_{k'=1}^{K}\hat{\chi}_{k'}\right)\right] +m^2L^{-1}b_1\left(\frac{\bar{p}_s}{K}\right)\sum_{k'=1}^{K}\hat{\chi}_{k'},$$

$$\hat{M}_k-\hat{M}_{k-1} = m^2L_1^{-1}a_k\left[-(\Delta\sigma)\tilde{\Gamma}_k\left(\sum_{k'=1}^{k}\hat{\chi}_{k'}-\frac{k}{K}\sum_{k'=1}^{K}\hat{\chi}_{k'}\right) +(\Delta\sigma)\tilde{\Gamma}_{k-2}\left(\sum_{k'=1}^{k-2}\hat{\chi}_{k'}-\frac{k-2}{K}\sum_{k'=1}^{K}\hat{\chi}_{k'}\right)\right] +m^2L^{-1}b_k\left(\frac{\bar{p}_s}{K}\right)\sum_{k'=1}^{K}\hat{\chi}_{k'}. \quad (43)$$

The above can also be written in matrix form as

$$E_1\tilde{M} = m^2L_1^{-1}A_\sigma\tilde{X} + m^2L^{-1}B_\sigma\tilde{X}, \quad (44)$$

where

$$\tilde{M}=\begin{pmatrix}\hat{M}_1\\ \hat{M}_2\\ \hat{M}_3\\ \hat{M}_4\\ .\\ .\\ .\\ \hat{M}_K\end{pmatrix}, \qquad \tilde{X}=\begin{pmatrix}\hat{\chi}_1\\ \hat{\chi}_2\\ \hat{\chi}_3\\ \hat{\chi}_4\\ .\\ .\\ .\\ \hat{\chi}_K\end{pmatrix},$$

$$E_1=\begin{pmatrix}1&0&0&0&\cdots&0&0\\ -1&1&0&0&\cdots&0&0\\ 0&-1&1&0&\cdots&0&0\\ 0&0&-1&1&\cdots&0&0\\ &&&&\cdots&&\\ &&&&\cdots&&\\ &&&&\cdots&&\\ 0&0&0&0&\cdots&-1&1\end{pmatrix},$$

and A_σ and B_σ are again matrices whose elements are also determined by the vertical stratification of the basic state.

Eliminating $\tilde{M}$ from (42) and (44) leads to:

$$\frac{1}{m^2}(L^2+f_0^2)\tilde{X}+(E_1^{-1}B_\sigma)\tilde{X} +(LL_1^{-1})(C_\sigma+E_1^{-1}A_\sigma)\tilde{X}=0, \quad (45)$$

i.e.,

$$\frac{1}{m^2}\left(\left[\frac{\Lambda-1}{\tau_1\Lambda+\tau_2}\right]^2+f_0^2\right)\tilde{X}+(E_1^{-1}B_\sigma)\tilde{X} +\left(\frac{\tilde{\tau}_1\Lambda+\tilde{\tau}_2+\tilde{\tau}_3\Lambda^{-1}}{\tau_1\Lambda+\tau_2}\right)(C_\sigma+E_1^{-1}A_\sigma)\tilde{X}=0. \quad (46)$$

In the case where the potential temperature is decomposed into its horizontal mean and perturbation parts and the vertical advection associated with the mean is treated implicitly, we have $(\tilde{\tau}_1,\tilde{\tau}_2,\tilde{\tau}_3)=(\tau_1,\tau_2,0)$. Therefore, eq. (46) becomes:

$$\frac{1}{m^2}\left(\left[\frac{\Lambda-1}{\tau_1\Lambda+\tau_2}\right]^2+f_0^2\right)\tilde{X}+D_\sigma\tilde{X}=0, \quad (47)$$

where $D_\sigma = C_\sigma + E^{-1}(A_\sigma+B_\sigma)$. Denoting the eigenvalues of D_σ as λ_k $(k=1,2,3,\ldots,K)$, the solutions for Λ can be written as:

$$\Lambda_k=\frac{1\pm i(1-\varepsilon)\,[(\tau f_0)^2+\tau^2m^2\lambda_k]^{1/2}}{1\mp i(1+\varepsilon)[(\tau f_0)^2+\tau^2m^2\lambda_k]^{1/2}}, \quad (48)$$

where $\tau=\Delta t/2$. Clearly the model gravity–inertia waves are neutrally stable in the case of no uncentering ($\varepsilon=0.0$) and stable when uncentering is present ($\varepsilon>0$).

In the case where the thermodynamic equation is SLSI discretized in a straightforward manner, i.e., $\theta^{n+1}=\theta_*^n$, with the departure points estimated using an extrapolated velocity, we have $(\tilde{\tau}_1,\tilde{\tau}_2,\tilde{\tau}_3)=(0,\frac{3}{2},-\frac{1}{2})\Delta t$. The solution for Λ will

then not be in as clean a form as (48). Also, the numerical stability is not ensured. Though it is not clear whether instability is sure to arise, the additional roots (due to the equation for Λ being cubic instead of quadratic) imply extra modes, leading at least to undesirable computational noise if not to fatal numerical instability.

4. Numerical results

The model has 64 grid-points in the zonal direction and 33 grid-points in the meridional direction including the 2 poles (i.e., a 5.29×5.29 degree resolution). There are 18 layers in the vertical, which are equally spaced in σ. The time-step is chosen as one hour. The multigrid solver that can handle cases in which the vertical coordinate is either σ or θ has been developed. For the experiments discussed in this paper, no uncentering has been used though it is an option in the model code. Thus far, no experiments with the vertical coordinate specified as of hybrid $\sigma - \theta$ have been carried out. We present only results with the σ-coordinate and leave the θ-coordinate to a future paper when the multigrid solver for the generalized vertical coordinate is available.

The first experiment is a simulation of developing baroclinic waves. The specification of the initial condition follows that described in the Appendix A of Pierce et al. (1991). In order to enhance the baroclinicity, the parameter A is chosen to be 4.5 instead of 2.5. The mean surface pressure is 1000 hPa and the pressure at the top is 50 hPa. The zonal wave number (4) and the other parameters are also the same as in Pierce et al. The vertical profiles of the zonal mean of the initial potential temperature and zonal velocity are shown in Fig. 2a. The frontal zones are centered at 45°. As a result of geostrophic balance, 2 zonal jets are located above the 2 frontal zones. Fig. 3a shows the initial surface pressure and potential temperature. Clearly, the initial perturbation with an amplitude of 1 hPa for the surface pressure is rather weak. These perturbations develop and evolve into cyclones and anticyclones with the associated development of cold/warm fronts. The maximum strength is reached around day 18 of which the surface pressure and potential temperature are shown in Fig. 3b. The development of these waves draws energy from the baroclinic mean state, which leads to dilution of the mean zonal fronts as well as the weakening of the jets as shown in Fig. 2b. More experiments with various degrees of baroclinicity and different sizes of amplitude for the initial perturbations also give consistent and reasonable results.

5. Conclusion and discussion

As mentioned above, the fact that PV is a most important dynamical quantity has led to the efforts of developing numerical models using PV as a direct model variable, as can be seen from the work based on shallow water equations (Bates et al., 1995; Bates and Li, 1996; Tolstykh, 1996; Thuburn, 1997). To the best of our knowledge, there have so far been no documented successes in extending the approach to 3D. Due to the problem of the isentropic PV (IPV) possibly becoming ill-defined in atmospheric boundary layers, PV cannot be used as a model variable in a straightforward manner. We have proposed in this paper a formulation to circumvent this problem. A so-called pseudo-PV (PPV) as well as the equation for it (PPV-equation) have been derived by using a generalized vertical coordinate that is to be specified as the terrain following σ (a function of σ in practice) in the lower layers and smoothly changes to θ above (again, a function of θ in practice). PPV reduces to IPV in the θ regions and thus retains the conservation property. In the lower layers where the vertical stratification can possibly become neutral and even slightly unstable, PPV is still well-defined, but not a conserved quantity any more. In the real atmosphere, the conservation property of PV is rather poor in this region in any case. Therefore, using a non-conserved quantity (PPV) is not a disadvantage.

The linear stability analysis of the gravity–inertia waves indicates the need to separate the potential temperature into horizontal mean and perturbation parts, in order to facilitate an implicit treatment on the vertical advection associated with the mean part. The numerical experiments with the developing baroclinic waves give reasonable results and thus suggest that the proposed model formulation is feasible. When a fully developed multigrid solver is available, we will

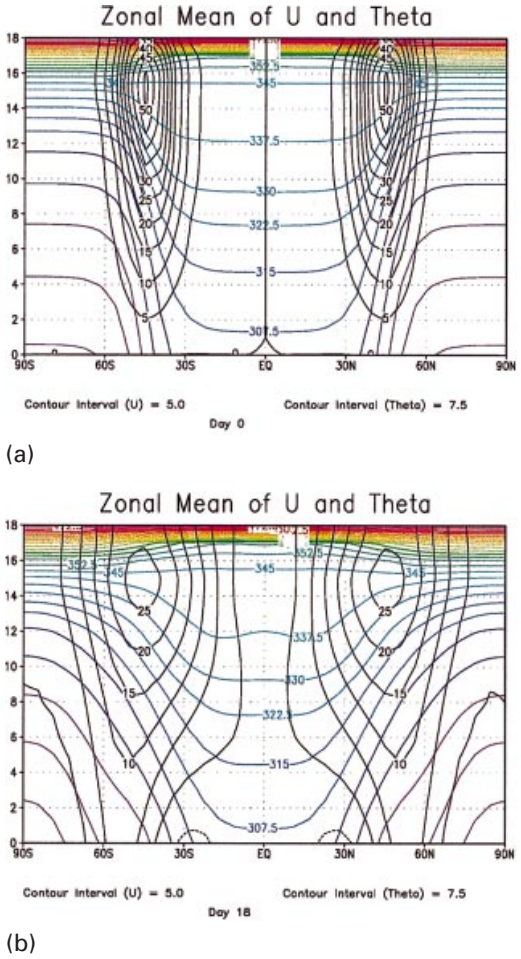

Fig. 2. Vertical cross-section of zonally averaged potential temperature and zonal velocity. The contour interval for the potential temperature is 7.5 K; the contour interval for the zonal velocity is 5 m/s. (a) Initial time; (b) day 18. (The pressure at the bottom of the model domain is 1000 hPa and at the top 50 hPa. The vertical gridding is uniform with equal grid interval based on σ.)

conduct a more comprehensive suite of experiments, and results will be reported in due course. It also remains to be proved that the model works properly when orography and model physics are included.

6. Acknowledgements

We have benefited from the discussions with B. J. Hoskins, D. R. Johnson, R. B. Pierce, C. S. Konor, S. E. Cohn, A. Staniforth, M. Rancic and J. Purser. Special thanks are due to S. F. McCormick who helped greatly on the managerial aspect of this collaborative work. Thanks are also due to the two anonymous reviewers whose comments have helped improve the quality of the manuscript. This research was supported by NASA grants 578-41-16-20. At the last stage of writing, YL was also affiliated with the Danish Center for Earth System Science supported by The Danish National Research Foundation.

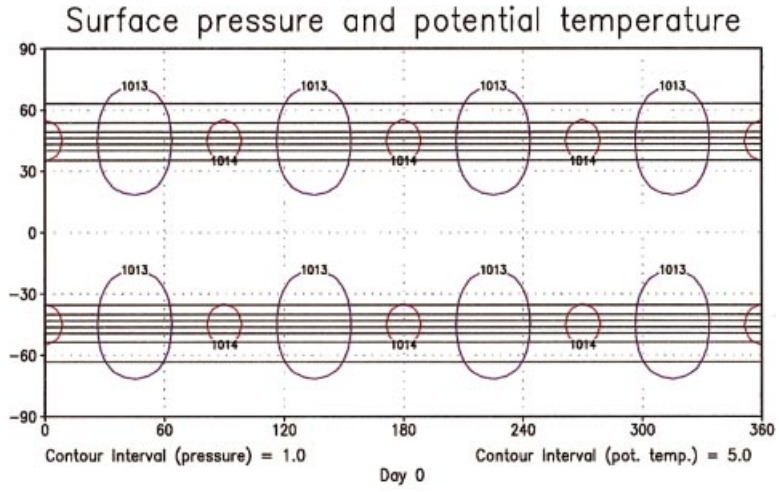

(a)

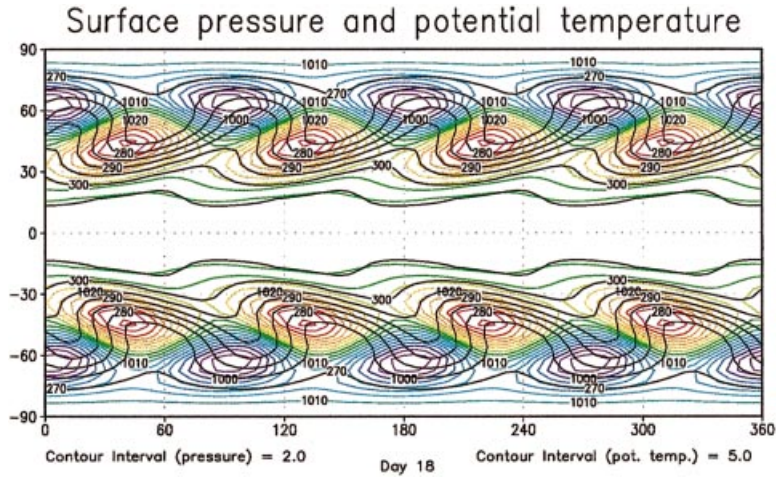

(b)

Fig. 3. Surface pressure and potential temperature. (a) Initial time (the contour interval for the surface pressure is 1.0 hPa; the contour interval for the surface potential temperature is 5.0 K); (b) day 18 (the contour interval for the surface pressure is 2.0 hPa; the contour interval for the surface potential temperature is 5.0 K).

REFERENCES

Arakawa, A. and Moorthi, S. 1988. Baroclinic instability in vertically discrete systems. *J. Atmos. Sci.* **45**, 1688–1707.

Arakawa, A. and Konor, C. S. 1996. Vertical differencing of the primitive equations based on the Charney–Phillips grid in hybrid σ–p vertical coordinates. *Mon. Wea. Rev.* **124**, 511–528.

Bates, J. R. and McDonald, A. 1982. Multiply-upstream, semi-Lagrangian advective schemes: analysis and application to a multilevel primitive equation model. *Mon. Wea. Rev.* **110**, 1831–1842.

Bates, J. R., Semazzi, F. H. M., Higgins, R. W. and Barros, S. R. M. 1990. Integration of the shallow water equations on the sphere using a vector semi-Lagrangian scheme with a multigrid solver. *Mon. Wea. Rev.* **118**, 1615–1627.

Bates, J. R., Li, Y., Brandt, A., McCormick, S. F. and Ruge, J. 1995. A global shallow-water numerical model

based on the semi-Lagrangian advection of potential vorticity. *Q. J. R. Meteorol. Soc.* **121**, 1981–2005.

Bleck, R. and Benjamin, S. G. 1993. Regional weather prediction with a model combining terrain-following and isentropic coordinates (I). Model description. *Mon. Wea. Rev.* **121**, 1770–1785.

Brandt, A. 1977. Multi-level adaptive solutions to boundary-value problems. *Math. Comp.* **31**, 333–390.

Brandt, A. 1988. Multi-level computations: review and recent developments. In: *Multigrid methods: theory, applications and supercomputing* (ed. McCormick, S. F), pp. 35–62. Marcel Dekker Inc., New York and Basel.

Charney, J. G. 1962. Integration of the primitive and balance equations. In: *Proceedings of the International Symposium on Numerical weather prediction.* Tokyo, Nov. 1960, Meteorological Society of Japan.

Charney, J. G. and Phillips, N. A. 1953. Numerical integration of the quasi-geostrophic equation for barotropic and simple baroclinic flows. *J. Meteor.* **10**, 71–99.

Ertel, H. 1942. Ein neuer hydrodynamischer Wirbelsatz. *Met. Zeitsch.* **59**, 271–281.

Hoskins, B. J., McIntyre, M. E. and Robertson, A. W. 1985. On the use and significance of isentropic potential vorticity maps. *Q. J. R. Meteorol. Soc.* **111**, 877–946.

Hsu, Y-J. G. and Arakawa, A. 1990. Numerical modeling of the atmosphere with an isentropic vertical coordinate. *Mon. Wea. Rev.* **118**, 1933–1959.

Johnson, R. D., Zapotocny, T. H., Reames, F. M., Wolf, B. J. and Pierce, R. B. 1993. A comparison of simulated precipitation by hybrid isentropic-sigma and sigma models. *Mon. Wea. Rev.* **121**, 2088–2114.

Kasahara, A. 1974. Various vertical coordinate systems used for numerical weather prediction. *Mon. Wea. Rev.* **102**, 509–522.

Konor, C. S. and Arakawa, A. 1997. Design of an atmospheric model based on a generalized vertical coordinate. *Mon. Wea. Rev.* **125**, 1649–1673.

Li, Y. and Bates, J. R. 1996. A study of the behaviour of semi-Lagrangian models in the presence of orography. *Quart. J. R. Met. Soc.* **122**, 1675–1700.

Li, Y., Ménard, R., Riishøjgaard, L.-P., Cohn, S. E. and Rood, R. B. 1998. A study on assimilating potential vorticity data. *Tellus* **50A**, 490–506.

Lorenz, E. N. 1960. Energy and numerical weather prediction. *Tellus* **12**, 364–373.

McCormick, S. F. 1992. *Multilevel projection methods in partial differential equations.* CBMS-NSF Series, SIAM, Philadelphia.

Pierce, R. B., Johnson, D. R., Reames, F. M., Zapotocny, T. H. and Wolf, B. J. 1991. Numerical investigations with a hybrid isentropic-sigma model. Part 1: normal-mode characteristics. *J. Atmos. Sci.* **48**, 2005–2024.

Rivest, C., Staniforth, A. and Robert, A. 1994. Spurious resonant response of semi-Lagrangian discretizations to orographic forcing: diagnosis and solution. *Mon. Wea. Rev.* **122**, 366–376.

Robert, A. 1981. A stable numerical integration scheme for the primitive meteorological equations. *Atmos. Ocean* **19**, 35–46.

Robert, A. 1982. A semi-Lagrangian and semi-implicit numerical integration scheme for the primitive meteorological equations. *J. Meteor. Soc. Japan* **60**, 319–325.

Rossby, C. G. 1936. Dynamics of steady ocean currents in the light of experimental fluid dynamics. *Papers in Physical oceanography and meteorology*, vol. 1, no. 1. Massachusetts Institute of Technology and Woods Hole Oceanographic Institution.

Staniforth, A. and Côté, J. 1991. Semi-Lagrangian integration schemes for atmospheric models — a review. *Mon. Wea. Rev.* **119**, 2206–2223.

Temperton, C. and Staniforth, A. 1987. An efficient two-time-level semi-Lagrangian semi-implicit integration scheme. *Q. J. R. Meteorol. Soc.* **113**, 1025–1039.

Thuburn, J. 1997. A PV-based shallow water model on a hexagonal-icosahedral grid. *Mon. Wea. Rev.* **125**, 2328–2350.

Tolstykh, M. 1996. Global semi-Lagrangian atmospheric model based on compact finite differences. Proceedings of the ECCOMAS 96 Conference (European Computational Fluid Dynamics Conference 1996), pp. 1–6. Published by John Wiley and Sons, Ltd.

Zhu, Z., Thuburn, J., Hoskins, B. J. and Haynes, P. H. 1992. A vertical finite-difference scheme based on a hybrid σ–θ–p coordinate. *Mon. Wea. Rev.* **120**, 851–862.